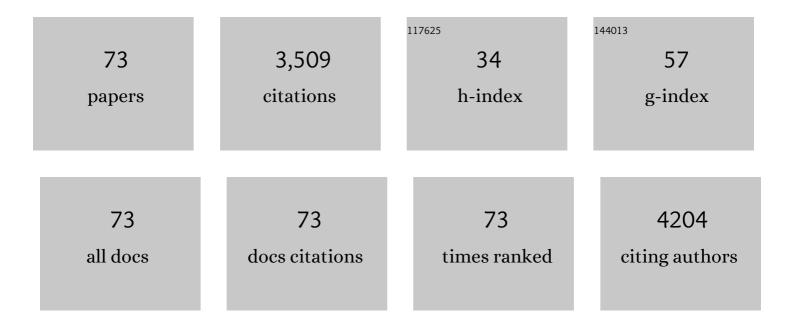
## List of Publications by Year in descending order

Source: https://exaly.com/author-pdf/4206483/publications.pdf Version: 2024-02-01



MENC XIE

#	Article	IF	CITATIONS
1	Synthesis of magnetic CoFe2O4/g-C3N4 composite and its enhancement of photocatalytic ability under visible-light. Colloids and Surfaces A: Physicochemical and Engineering Aspects, 2015, 478, 71-80.	4.7	253
2	Novel magnetic CoFe 2 O 4 /Ag/Ag 3 VO 4 composites: Highly efficient visible light photocatalytic and antibacterial activity. Applied Catalysis B: Environmental, 2016, 199, 11-22.	20.2	211
3	Constructing magnetic catalysts with in-situ solid-liquid interfacial photo-Fenton-like reaction over Ag3PO4@NiFe2O4 composites. Applied Catalysis B: Environmental, 2018, 225, 40-50.	20.2	175
4	Construction of novel CNT/LaVO4 nanostructures for efficient antibiotic photodegradation. Chemical Engineering Journal, 2019, 357, 487-497.	12.7	158
5	Three dimensional polyaniline/MgIn2S4 nanoflower photocatalysts accelerated interfacial charge transfer for the photoreduction of Cr(VI), photodegradation of organic pollution and photocatalytic H2 production. Chemical Engineering Journal, 2019, 360, 1601-1612.	12.7	142
6	Core–shell structured Fe3O4@TiO2-doxorubicin nanoparticles for targeted chemo-sonodynamic therapy of cancer. International Journal of Pharmaceutics, 2015, 486, 380-388.	5.2	137
7	Different Morphologies of SnS <sub>2</sub> Supported on 2D g-C <sub>3</sub> N <sub>4</sub> for Excellent and Stable Visible Light Photocatalytic Hydrogen Generation. ACS Sustainable Chemistry and Engineering, 2018, 6, 5132-5141.	6.7	125
8	A multifunctional mesoporous silica nanocomposite for targeted delivery, controlled release of doxorubicin and bioimaging. Colloids and Surfaces B: Biointerfaces, 2013, 110, 138-147.	5.0	108
9	Surface modification of graphene oxide nanosheets by protamine sulfate/sodium alginate for anti-cancer drug delivery application. Applied Surface Science, 2018, 440, 853-860.	6.1	101
10	Direct Z-scheme red carbon nitride/rod-like lanthanum vanadate composites with enhanced photodegradation of antibiotic contaminants. Applied Catalysis B: Environmental, 2020, 277, 119245.	20.2	90
11	Sulfur promoted n-ï€* electron transitions in thiophene-doped g-C3N4 for enhanced photocatalytic activity. Chinese Journal of Catalysis, 2021, 42, 450-459.	14.0	87
12	Visible-light-driven Ag/AgBr/ZnFe2O4 composites with excellent photocatalytic activity for E. coli disinfection and organic pollutant degradation. Journal of Colloid and Interface Science, 2018, 512, 555-566.	9.4	84
13	Layer-by-layer modification of magnetic graphene oxide by chitosan and sodium alginate with enhanced dispersibility for targeted drug delivery and photothermal therapy. Colloids and Surfaces B: Biointerfaces, 2019, 176, 462-470.	5.0	79
14	Non-covalent modification of graphene oxide nanocomposites with chitosan/dextran and its application in drug delivery. RSC Advances, 2016, 6, 9328-9337.	3.6	69
15	Chitosan/sodium alginate modificated graphene oxide-based nanocomposite as a carrier for drug delivery. Ceramics International, 2016, 42, 17798-17805.	4.8	62
16	In situ construction efficient visible-light-driven three-dimensional Polypyrrole/Zn3In2S6 nanoflower to systematically explore the photoreduction of Cr(VI): Performance, factors and mechanism. Journal of Hazardous Materials, 2020, 384, 121480.	12.4	61
17	Synthesis of zinc ferrite/silver iodide composite with enhanced photocatalytic antibacterial and pollutant degradation ability. Journal of Colloid and Interface Science, 2018, 528, 70-81.	9.4	58
18	Magnetically separable Fe2O3/g-C3N4 catalyst with enhanced photocatalytic activity. RSC Advances, 2015, 5, 95727-95735.	3.6	57

#	Article	IF	CITATIONS
19	Enhanced long-wavelength light utilization with polyaniline/bismuth-rich bismuth oxyhalide composite towards photocatalytic degradation of antibiotics. Journal of Colloid and Interface Science, 2019, 537, 101-111.	9.4	53
20	Cobalt phosphide nanoparticles embedded in 3D N-doped porous carbon for efficient hydrogen and oxygen evolution reactions. International Journal of Hydrogen Energy, 2019, 44, 4543-4552.	7.1	52
21	High yield synthesis of nano-size g-C <sub>3</sub> N <sub>4</sub> derivatives by a dissolve-regrowth method with enhanced photocatalytic ability. RSC Advances, 2015, 5, 26281-26290.	3.6	51
22	Promoting LED light driven photocatalytic inactivation of bacteria by novel β-Bi2O3@BiOBr core/shell photocatalyst. Journal of Alloys and Compounds, 2020, 816, 152665.	5.5	47
23	Negative-charge-functionalized mesoporous silica nanoparticles as drug vehicles targeting hepatocellular carcinoma. International Journal of Pharmaceutics, 2014, 474, 223-31.	5.2	46
24	Ni3Fe nanoparticles enclosed by B-doped carbon for efficient bifunctional performances of oxygen and hydrogen evolution reactions. Journal of Alloys and Compounds, 2020, 835, 155267.	5.5	46
25	Novel Ag <sub>2</sub> S quantum dot modified 3D flower-like SnS <sub>2</sub> composites for photocatalytic and photoelectrochemical applications. Inorganic Chemistry Frontiers, 2018, 5, 63-72.	6.0	43
26	An efficient broad spectrum-driven carbon and oxygen co-doped g-C3N4 for the photodegradation of endocrine disrupting: Mechanism, degradation pathway, DFT calculation and toluene selective oxidation. Journal of Hazardous Materials, 2021, 401, 123309.	12.4	43
27	Multifunctional C-Doped CoFe <sub>2</sub> O <sub>4</sub> Material as Cocatalyst to Promote Reactive Oxygen Species Generation over Magnetic Recyclable C–CoFe/Ag–AgX Photocatalysts. ACS Sustainable Chemistry and Engineering, 2018, 6, 11968-11978.	6.7	42
28	A core–shell structured magnetic Ag/AgBr@Fe <sub>2</sub> O <sub>3</sub> composite with enhanced photocatalytic activity for organic pollutant degradation and antibacterium. RSC Advances, 2015, 5, 71035-71045.	3.6	41
29	A Z-scheme magnetic recyclable Ag/AgBr@CoFe <sub>2</sub> O <sub>4</sub> photocatalyst with enhanced photocatalytic performance for pollutant and bacterial elimination. RSC Advances, 2017, 7, 30845-30854.	3.6	40
30	Nickel and cobalt in situ grown in 3-dimensional hierarchical porous graphene for effective methanol electro-oxidation reaction. Journal of Electroanalytical Chemistry, 2019, 838, 7-15.	3.8	40
31	Construction of polythiophene/Bi4O5I2 nanocomposites to promote photocatalytic degradation of bisphenol a. Journal of Alloys and Compounds, 2020, 823, 153773.	5.5	39
32	Porous defective carbon nitride obtained by a universal method for photocatalytic hydrogen production from water splitting. Journal of Colloid and Interface Science, 2020, 566, 171-182.	9.4	39
33	Novel broad-spectrum-driven oxygen-linked band and porous defect co-modified orange carbon nitride for photodegradation of Bisphenol A and 2-Mercaptobenzothiazole. Journal of Hazardous Materials, 2020, 396, 122659.	12.4	36
34	Ag <sub>2</sub> S quantum dots in situ coupled to hexagonal SnS <sub>2</sub> with enhanced photocatalytic activity for MO and Cr( <scp>vi</scp> ) removal. RSC Advances, 2017, 7, 46823-46831.	3.6	35
35	Novel broad spectrum light responsive PPy/hexagonal-SnS2 photocatalyst for efficient photoreduction of Cr(VI). Materials Research Bulletin, 2019, 112, 226-235.	5.2	35
36	Cobalt–Iron nanoparticles encapsulated in mesoporous carbon nanosheets: A one-pot synthesis of highly stable electrocatalysts for overall water splitting. International Journal of Hydrogen Energy, 2021, 46, 5234-5249.	7.1	35

#	Article	IF	CITATIONS
37	Preparation of magnetic Ag/AgCl/CoFe <sub>2</sub> O <sub>4</sub> composites with high photocatalytic and antibacterial ability. RSC Advances, 2015, 5, 41475-41483.	3.6	32
38	Core–shell magnetic Ag/AgCl@Fe <sub>2</sub> O <sub>3</sub> photocatalysts with enhanced photoactivity for eliminating bisphenol A and microbial contamination. New Journal of Chemistry, 2016, 40, 3413-3422.	2.8	32
39	Graphene oxide-modified LaVO <sub>4</sub> nanocomposites with enhanced photocatalytic degradation efficiency of antibiotics. Inorganic Chemistry Frontiers, 2018, 5, 2818-2828.	6.0	31
40	WS <sub>2</sub> nanosheets functionalized by biomimetic lipids with enhanced dispersibility for photothermal and chemo combination therapy. Journal of Materials Chemistry B, 2020, 8, 2331-2342.	5.8	31
41	Fabrication of magnetic BaFe <sub>12</sub> O <sub>19</sub> /Ag <sub>3</sub> PO <sub>4</sub> composites with an <i>in situ</i> photo-Fenton-like reaction for enhancing reactive oxygen species under visible light irradiation. Catalysis Science and Technology, 2019, 9, 2563-2570.	4.1	30
42	Layered MoS2 nanosheets modified by biomimetic phospholipids: Enhanced stability and its synergistic treatment of cancer with chemo-photothermal therapy. Colloids and Surfaces B: Biointerfaces, 2020, 187, 110631.	5.0	30
43	Synergistically coupling of Co/Mo2C/Co6Mo6C2@C electrocatalyst for overall water splitting: The role of carbon precursors in structural engineering and catalytic activity. Applied Surface Science, 2022, 579, 152148.	6.1	29
44	3D graphene decorated with hexagonal micro-coin of Co(OH)2: A competent electrocatalyst for hydrogen and oxygen evolution reaction. International Journal of Hydrogen Energy, 2019, 44, 14770-14779.	7.1	28
45	Enhanced LED-light-driven photocatalytic antibacterial by g-C3N4/BiOI composites. Journal of Materials Science: Materials in Electronics, 2019, 30, 2783-2794.	2.2	28
46	Realizing the synergistic effect of electronic modulation over graphitic carbon nitride for highly efficient photodegradation of bisphenol A and 2-mercaptobenzothiazole: Mechanism, degradation pathway and density functional theory calculation. Journal of Colloid and Interface Science, 2021, 583, 113-127.	9.4	26
47	Construction of solid–liquid interfacial Fenton-like reaction under visible light irradiation over etched CoxFeyO4–BiOBr photocatalysts. Catalysis Science and Technology, 2018, 8, 551-561.	4.1	22
48	Nickel loaded graphene-like carbon sheets an improved electrocatalyst for hydrogen evolution reaction. Materials Chemistry and Physics, 2019, 227, 105-110.	4.0	22
49	Facile synthesis of N, S co-doped MoO2@C nanorods as an outstanding electrocatalyst for hydrogen evolution reaction. Applied Surface Science, 2021, 537, 147971.	6.1	21
50	Tailoring of crystalline structure of carbon nitride for superior photocatalytic hydrogen evolution. Journal of Colloid and Interface Science, 2019, 556, 324-334.	9.4	20
51	Chitosan and dextran stabilized GO-iron oxide nanosheets with high dispersibility for chemotherapy and photothermal ablation. Ceramics International, 2019, 45, 5996-6003.	4.8	19
52	Surface amorphous carbon doping of carbon nitride for efficient acceleration of electron transfer to boost photocatalytic activities. Applied Surface Science, 2020, 507, 145145.	6.1	19
53	Preparation of magnetically recoverable and Z-scheme BaFe12O19/AgBr composite for degradation of 2-Mercaptobenzothiazole and Methyl orange under visible light. Applied Surface Science, 2020, 521, 146343.	6.1	19
54	The construction of a Fenton system to achieve in situ H2O2 generation and decomposition for enhanced photocatalytic performance. Inorganic Chemistry Frontiers, 2019, 6, 1490-1500.	6.0	18

#	Article	IF	CITATIONS
55	Incorporation of pyridinic and graphitic N to Ni@ <scp>CNTs</scp> : As a competent electrocatalyst for hydrogen evolution reaction. International Journal of Energy Research, 2020, 44, 9157-9165.	4.5	18
56	An erythrocyte membrane-camouflaged biomimetic nanoplatform for enhanced chemo-photothermal therapy of breast cancer. Journal of Materials Chemistry B, 2022, 10, 2047-2056.	5.8	18
57	Hierarchical Co/MoO2@N-doped carbon nanosheets derived from waste lotus leaves for electrocatalytic water splitting. International Journal of Hydrogen Energy, 2022, 47, 15673-15686.	7.1	18
58	Ni-Fe-Co based mixed metal/metal-oxides nanoparticles encapsulated in ultrathin carbon nanosheets: A bifunctional electrocatalyst for overall water splitting. Surfaces and Interfaces, 2021, 26, 101361.	3.0	17
59	B-doped carbon enclosed Ni nanoparticles: A robust, stable and efficient electrocatalyst for hydrogen evolution reaction. Journal of Electroanalytical Chemistry, 2020, 869, 114085.	3.8	16
60	C–O band structure modified broad spectral response carbon nitride with enhanced electron density in photocatalytic peroxymonosulfate activation for bisphenol pollutants removal. Journal of Hazardous Materials, 2022, 432, 128663.	12.4	16
61	In situ growth of Ag/AgCl on the surface of CNT and the effect of CNT on the photoactivity of the composite. New Journal of Chemistry, 2015, 39, 5540-5547.	2.8	15
62	Hierarchical ultrathin defect-rich CoFe <sub>2</sub> O <sub>4</sub> @BC nanoflowers synthesized <i>via</i> a temperature-regulated strategy with outstanding hydrogen evolution reaction activity. Inorganic Chemistry Frontiers, 2021, 8, 1455-1467.	6.0	14
63	Modification of magnetic molybdenum disulfide by chitosan/carboxymethylcellulose with enhanced dispersibility for targeted photothermal-/chemotherapy of cancer. Journal of Materials Chemistry B, 2021, 9, 1833-1845.	5.8	14
64	Novel 3D graphene ornamented with CoO nanoparticles as an efficient bifunctional electrocatalyst for oxygen and hydrogen evolution reactions. Materials Chemistry and Physics, 2021, 261, 124237.	4.0	14
65	Probing effective charge migration and highly improved photocatalytic activity on Polyaniline/Zn3In2S6 nano-flower under long wavelength light. Separation and Purification Technology, 2021, 274, 119004.	7.9	14
66	The camouflage of graphene oxide by red blood cell membrane with high dispersibility for cancer chemotherapy. Journal of Colloid and Interface Science, 2021, 591, 290-299.	9.4	13
67	Highly Stable Ultrafine Boronâ€Doped NiCo@Carbon Nanoparticles as a Robust Electrocatalyst for the Hydrogen Evolution Reaction. ChemElectroChem, 2021, 8, 1337-1348.	3.4	8
68	Ni nanoparticles oriented on MoO2@BC nanosheets with an outstanding long-term stability for hydrogen evolution reaction. Chemical Engineering Science, 2021, 246, 116868.	3.8	8
69	Development of a magnetic MoS2 system camouflaged by lipid for chemo/phototherapy of cancer. Colloids and Surfaces B: Biointerfaces, 2022, 213, 112389.	5.0	8
70	Simultaneous fabrication of cobaltâ€based graphene with rich N dopant for hydrogen evolution reaction in basic medium. International Journal of Energy Research, 2021, 45, 14010-14020.	4.5	7
71	Angstrom-sized tungsten carbide promoted platinum electrocatalyst for effective oxygen reduction reaction and resource saving. RSC Advances, 2015, 5, 96488-96494.	3.6	6
72	Prostate cancer biomarker citrate detection using triaminoguanidinium carbon dots, its applications in live cells and human urine samples. Spectrochimica Acta - Part A: Molecular and Biomolecular Spectroscopy, 2022, 268, 120622.	3.9	5

#	Article	IF	CITATIONS
73	Simultaneous synthesis of bimetallic@3D graphene electrocatalyst for HER and OER. Frontiers of Materials Science, 2021, 15, 305-315.	2.2	3